SMA Observations of NGC253 at 690 GHz

Alison Peck (NRAO), Melanie Krips (IRAM), Sergio Martin (IRAM), Kazushi Sakamoto (ASIAA)

We present preliminary results of the first interferometric observations of the ^{12}CO(J=6-5) emission in NGC 253 using the Submillimeter Array. We compare the ^{12}CO(J=6-5) emission with pre-existing data on ^{12}CO(J=3-2), ^{12}CO(J=2-1) and ^{12}CO(J=1-0) in NGC 253 at similar angular resolutions. The ^{12}CO(J=6-5) emission is clearly detected along the disk of NGC 253, however no emission is detected close to the superbubbles which have been seen toward the edges of the disk in the lower-J CO transitions.

Line	Frequency (GHz)	Date (mm/yyyy)	Rms[a] (mJy)	Δv (km s^{-1})	Beam[b] ($''\times''$)	Type	Ref
^{12}CO(J=6–5)	691.473 (USB)	09/2007	7000	12	4".2×2".1	Mosaic	Krips et al, in prep
^{12}CO(J=3–2)	345.796 (LSB)	09/2007	100	12	5".8×4".5	Mosaic	Krips et al, in prep
^{12}CO(J=3–2)	345.796 (LSB)	09/2004	130	12	3".9×1".9	Mosaic	Sakamoto et al, 2011
^{12}CO(J=2–1)	230.538 (both)	2003-2005	30	12	1".7×1".5	Single-field	Sakamoto et al, 2006; 2011
^{12}CO(J=1–0)	115.271 (USB)	2011	4	12	3".7×2".7	Mosaic	ALMA Archive (2011.0.00172.S)

Details of the observations made for this project, and those used for comparison. Note that the 2nd and 3rd datasets listed here have been combined in the plots shown, and that the ALMA data were rereduced in CASA and GILDAS in the same fashion as the SMA datasets for this comparison.

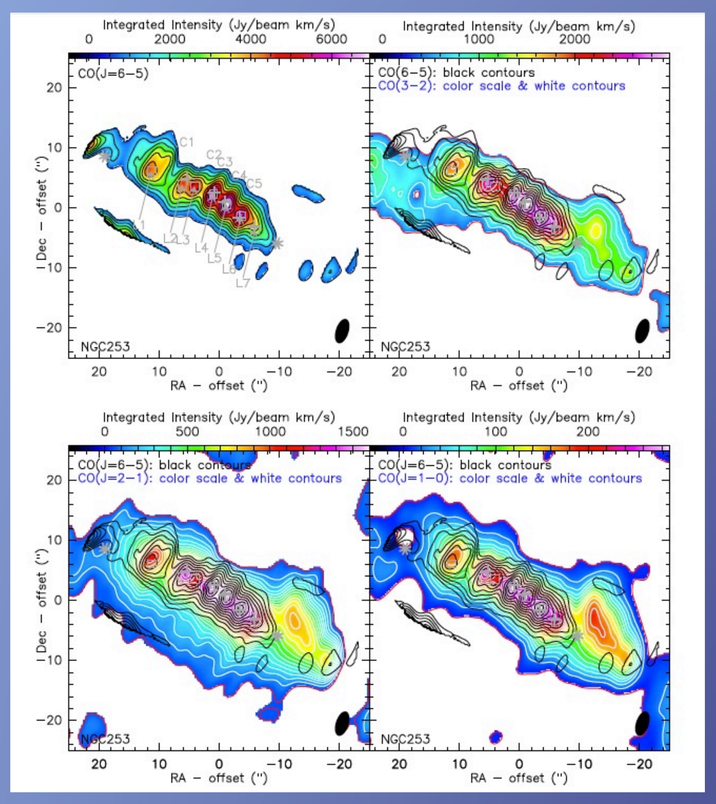

Above: Panels comparing the flux distributions of the four ^{12}CO line transitions. Panel 1 (upper left) shows the ^{12}CO(J=6–5) emission in color and contours. Panel 2 (upper right) shows the ^{12}CO(J=3–2) emission (from data taken for this project as well as that published in Sakamoto et al. (2011) overlaid with contours of the ^{12}CO(J=6–5) line emission. Panel 3 (lower left) shows the same but for the ^{12}CO(J=2–1) emission (taken from Sakamoto et al. 2011) overlaid with the contours of the ^{12}CO(J=6–5) emission. Panel 4 (lower right) shows the same but for the ^{12}CO(J=1–0) emission (taken from the ALMA science archive) overlaid with the contours of the ^{12}CO(J=6–5) emission. The grey crosses indicated in each panel mark the positions of the 1.3 mm continuum emission peaks from Sakamoto et al. (2011), the grey stars mark the positions of the two shells from Sakamoto et al. (2006) and L1-L7 (grey squares) with the corresponding arrows mark the line peaks of the ^{12}CO(J=6–5) emission in order to facilitate the discussion. The contours of the ^{12}CO(J=6–5) emission start at 2σ=660 Jy km s^{-1} beam^{-1} in steps of 2σ (all three panels). The contours of the ^{12}CO(J=3–2) emission start at 100σ=420 Jy km s^{-1} beam^{-1} in steps of 50σ (panel 2). The contours of the ^{12}CO(J=2–1) emission start at 50σ=64 Jy km s^{-1} beam^{-1} in steps of 50σ. The contours of the ^{12}CO(J=1–0) emission start at 25σ=5 Jy km s^{-1} beam^{-1} in steps of 75σ.

Designation	Position 00h47m (s)	Position −25°17′ (″)	S^{peak} (Jy beam^{-1})	I^{peak} (Jy beam^{-1} kms^{-1})	v_0 (km s^{-1})	FWHM (km s^{-1})
^{12}CO(6-5)						
L1	34.07	12.0	27.6±1.9	3948±438	−34±5	134±12
L2 (Sa1)	33.69	14.2	33.2±2.0	5206±499	−44±5	148±11
L3	33.54	14.5	29.3±2.0	5393±569	−50±6	173±14
L4 (Sa2)	33.31	15.8	40.9±2.0	7406±562	−15±4	170±10
L5 (Sa3)	33.15	17.5	40.1±1.8	6823±491	+7± 4	160± 9
L6 (Sa4)	32.97	19.4	47.3±2.1	5800±412	+32± 3	115± 6
L7 (Sa5)	32.80	21.7	26.4±2.4	2547±368	+38± 4	91±10
^{12}CO(1-0)						
L1	34.07	12.0	1.85±.03	179± 4	−40±1	91±1
L2 (Sa1)	33.69	14.2	1.56±.05	242±10	−60± 2	146±5
L3	33.54	14.5	1.25±.03	225± 9	−56± 2	170±5
L4 (Sa2)	33.31	15.8	1.71±.06	316±16	−38± 3	174±6
L5 (Sa3)	33.15	17.5	1.57±.05	314±16	−6± 3	189±7
L6 (Sa4)	32.97	19.4	2.37±.09	318±18	+17± 2	126±5
L7 (Sa5)	32.80	21.7	1.85±.06	217±11	+18± 2	110±4

Col 1: ^{12}CO(J=6–5) line emission peaks as designated in this work (starting with L) and the corresponding ^{12}CO(J=3–2) and ^{12}CO(J=2–1) names from Sakamoto et al. (2011).
Cols 2,3: Absolute position of each of the line emission peaks.
Cols 4,5: Fluxes and spectrally integrated intensities measured at the emission peak.
Col 6: Velocity offset relative to the LSR systemic velocity of 243 kms^{-1} for NGC 253.
Col 7: Full width at half maximum of each line.

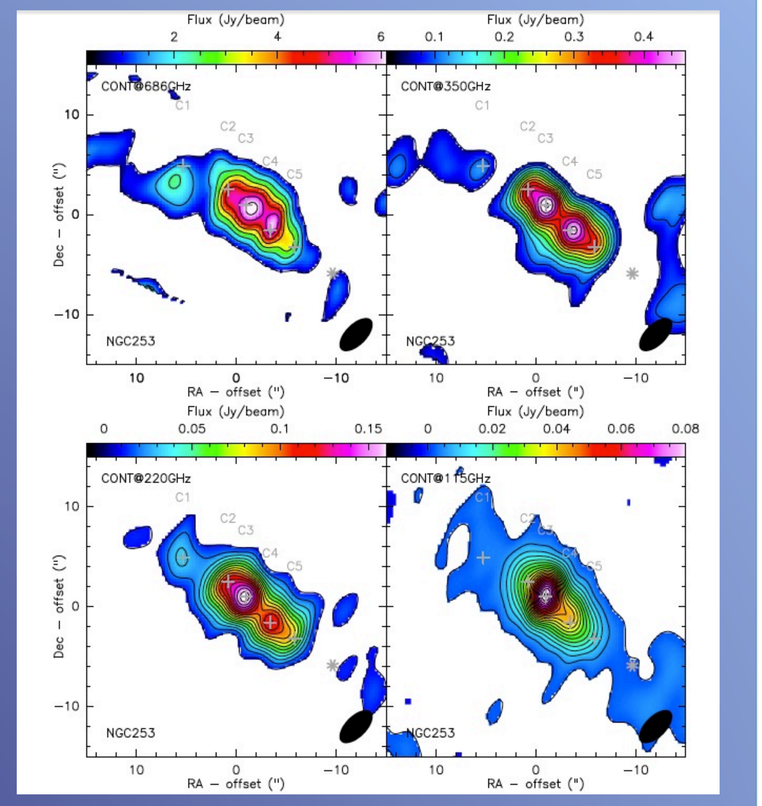

Above: Continuum emission at 686 GHz (panel 1, upper left), 350 GHz (panel 2, upper right), 220 GHz (panel 3, lower left) and 115 GHz (panel 4, lower right), all at an angular resolution of ~4".2x2".1. The contours of the 686 GHz continuum emission start at 2σ=0.76 Jy beam^{-1} in steps of 2σ, those of the 350 GHz continuum emission start at 10σ=0.064 Jy beam^{-1} and go in steps of 5σ, those of the 220 GHz continuum emission start at 5σ=0.01 Jy beam^{-1} and go in steps of 5σ, and those of the 115 GHz continuum emission start at 10σ=1.5 mJy beam^{-1} and go in steps of 25σ. The grey crosses in each panel mark the positions of the 1.3 mm continuum emission peaks from Sakamoto et al. (2011), the grey stars indicate the positions of superbubbles from Sakamoto et al. (2006).

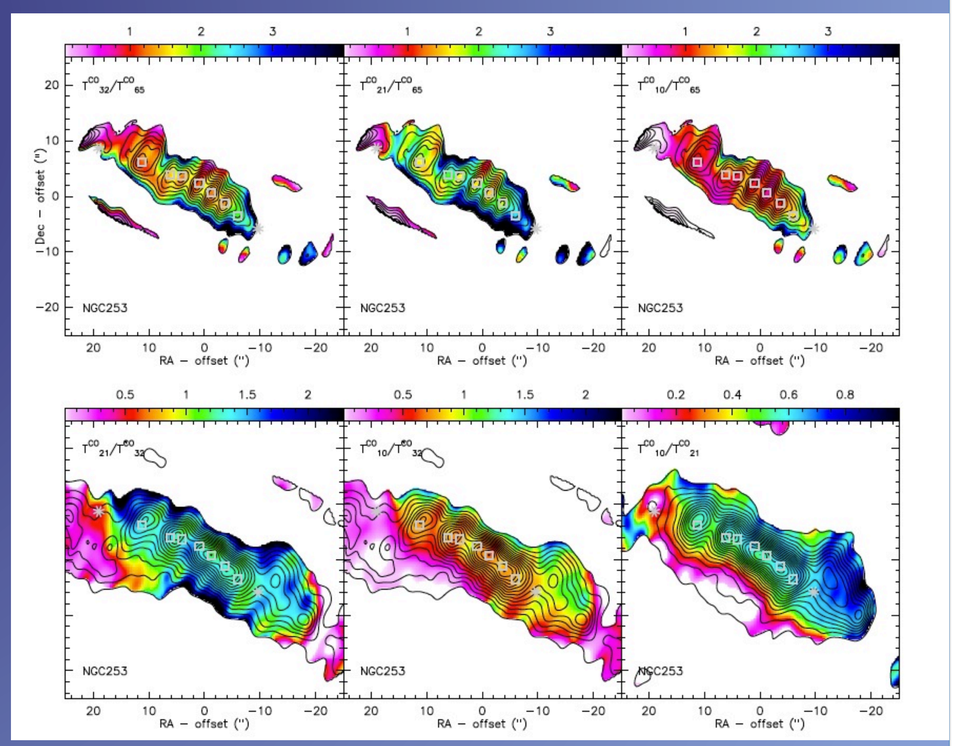

Above: Brightness temperature ratios between the various integrated ^{12}CO line transitions. The grey crosses are the same as in Fig. 4. Note that we used a reversed color scale in the sense that low ratios are represented as bright colors from white to red, while high ratios are represented with the darker blue and black shades. This was done to facilitate the connection between warm (and/or dense) molecular gas that is reflected here in low line ratios while cooler (and/or less dense) gas is shown by large line ratios.

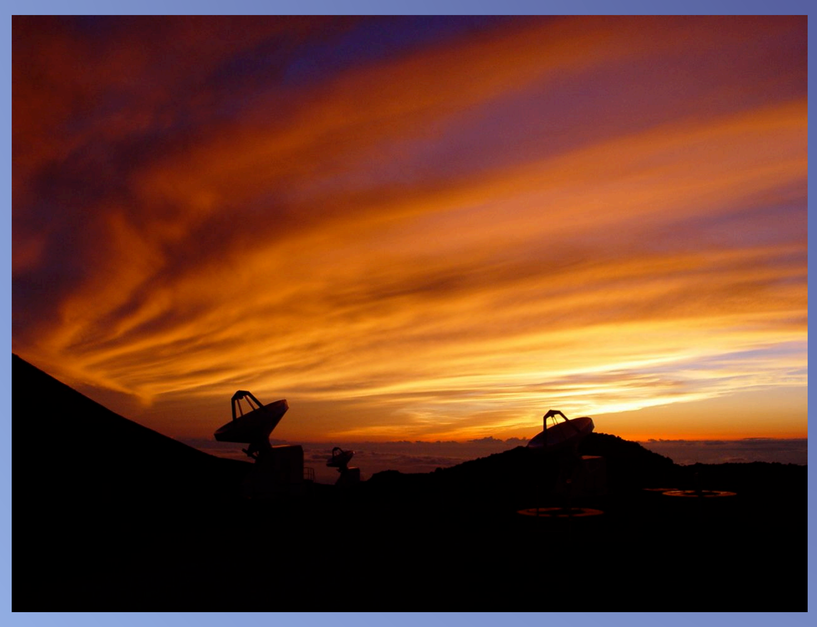

Right: The flux of the four different line transitions integrated over the entire emission region, as shown in the legend. It is clear from the broad profile that several emission components are present for each transition, indicating the presence of multiple molecular clouds or clumps at slightly different velocities. However, the extent of the velocity range is similar for each line, indicating that the gas is likely co-spatial in the clumps.

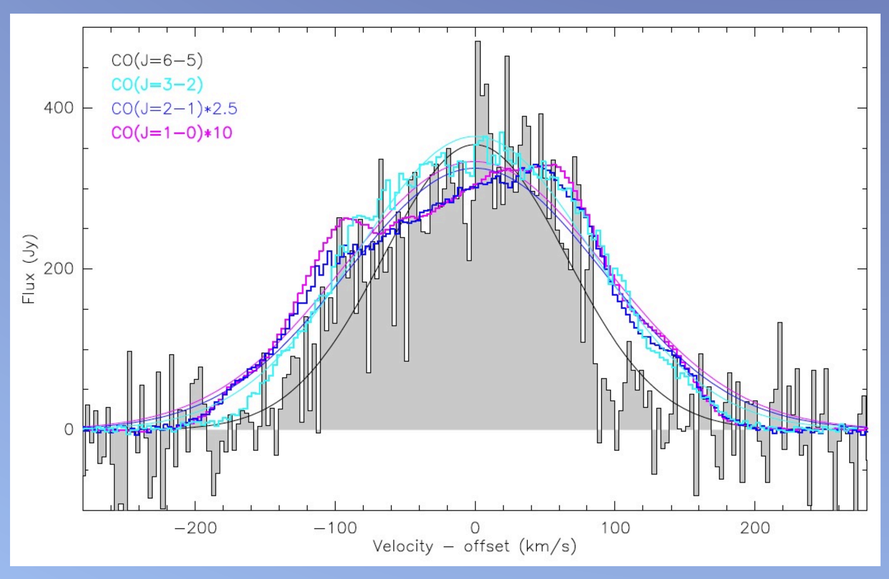

Below: Line spectra for the different peaks emission locations as labeled in the plot above left for each of the ^{12}CO transitions observed. A single-component Gaussian fit has been applied to all spectra. The results of these fits are shown in the central table.